

# Iranian Journal of Electrical and Electronic Engineering

Journal Homepage: ijeee.iust.ac.ir



# Design and Electromagnetic Analysis of a Novel Axial-Field Flux-Switching Permanent Magnet Machine Achieving Improved Torque Characteristics

Hamid Ebrahimi \*, Hossein Torkaman \*(C.A.), Alireza Sohrabzadeh \*, Hamid Javadi \*

**Abstract:** This paper introduces a unique rotor pole configuration for an Axial-Field Flux-Switching Permanent Magnet (AFFSPM) machine, focused on minimizing cogging torque (CT), reducing torque ripple (TR), and improving average torque (AT). This innovative design is based on the standard rotor configuration of the AFFSPM machine, with a Reversed Radial Pole (RRP) placement that this new topology will be recognized as RRPAFFSPM. To thoroughly evaluate the proposed design's effectiveness, sensitivity analysis will be conducted to determine the significance of geometric parameters and identify the best topology in comparison studies. Extensive 3D finite element analysis (FEA) confirms the design's effectiveness, demonstrating substantial reductions in CT and TR, along with an increase in AT. These results suggest that the desired rotor pole configuration is a promising solution for high-performance electric machines in demanding different applications.

**Keywords:** Axial Field, Flux Switching, Structural Modifications, Rotor Pole, 3D FEM.

# 1 Introduction

XIAL-FIELD flux-switching Permanent Magnet Amachines have become a viable alternative to traditional radial-field machines, especially applications that require high torque density, compactness, and efficiency [1]. Recently, these motors' topologies have garnered considerable attention for their unique abilities to combine the benefits of fluxswitching and axial flux path technologies, providing high torque/power density and reliability [2]. As a result, AFFSPM has found applications in various sectors, including electric vehicles (EVs) and renewable energy systems like wind turbines [3, 4]. The main challenges faced by AFFSPMs are CT and TR, which can significantly affect the motor's operational smoothness and efficiency [5]. Several design strategies have been investigated to address these issues, such as the modular combination technique and the optimization of pole shapes and rotor-stator configurations [6, 7], both of which have proven effective in reducing CT and enhancing torque uniformity [8]. **Dual-stator** configurations have also shown promise in reducing TR by balancing electromagnetic forces and smoothing overall torque production [9]. Performance evaluations, particularly in terms of efficiency and power density, have demonstrated the potential of AFFSPMs in various high-performance applications [10]. For instance, AFFSPMs with modular stators and flux-modulating rotors have exhibited excellent torque characteristics when optimized for wind energy applications [11]. Despite these advancements, challenges remain in the design of AFFSPMs, such as manufacturing complexity, material costs, and the impact of non-operational harmonics on electromagnetic performance [12, 13]. Various methods have been proposed in the literature to address these challenges [14]. For example, in [15], the impact of rotor parameters, including rotor pole number, pole width, pole shape, and rotor thickness, has been investigated and led to significant improvements, including a reduction in CT by approximately 40% and an increase in torque density by nearly 25%. The use of the design of experiments optimization method has resulted in a reduction of

1

Iranian Journal of Electrical & Electronic Engineering, 2026. Paper first received 14 Mar 2025 and accepted 05 Aug 2025.

Corresponding Author: Hossein Torkaman.

E-mail: <u>h\_torkaman@sbu.ac.ir</u>

This is an invited paper from ICEMD 2024 conference [35].

<sup>\*</sup> The authors are with the Faculty of Electrical Engineering, Shahid Beheshti University, Tehran, Iran.

approximately 62% in CT. The same study has been done in [16]. The E-core and U-core dual-stator modular motor, based on the flux modulation principle as presented in, showed significant torque improvements, including a 35-45% reduction in CT, a 30-40% decrease in TR, and a 20-25% increase in torque density [6]. The U-core design outperformed the E-core in terms of efficiency and mechanical vibration reduction. This study also emphasized the importance of stator/rotor pole combinations, with higher pole combinations yielding optimal torque density and smoother operation. The importance of stator core shape can also be found in [17, 18]. According to [19], combining dual rotors with hybrid excitation allows better control over flux paths, significantly reducing TR. Various methods have been proposed and reviewed, with detailed numerical reports on techniques such as adding magnetic bridges, teeth pairing, and various displacement methods, as discussed in [20-22]. The teeth skewing method in the rotor teeth discussed in [23] where three rotor teeth structures including fan-shaped, single-skew, and dual-skew are analyzed. The implementation of the rotor notching technique in [24] resulted in a 72% reduction in CT amplitude.

The rising demand for sustainable and efficient motor technologies in electric transportation highlights the need to optimize the performance, reliability, and safety of these machines [25]. In this context, TR and CT are critical factors that require attention [26]. Factors such as magnet strength, air-gap length, skew degree, and slot opening width influence this torque, which is typically expressed as a percentage of the peak torque [27].

CT can cause increased noise and vibration in electrical machines. In applications where low noise and vibration are essential, such as electric vehicles (EVs) [28], CT is undesirable and must be minimized [29]. This phenomenon directly affects efficiency, power density, and thermal management, all crucial for enhancing vehicle range, endurance, and overall performance [30]. Additionally, the impact of TR and CT extends to durability, reliability, and integration aspects, necessitating comprehensive solutions that address these issues while ensuring compatibility with existing infrastructure and vehicle architecture.

Therefore, while TR and CT present significant challenges, effectively managing them is key to unlocking the full potential of electrical machines in transportation applications.

Regarding this target, this paper investigates a new structural modification on the rotor pole to nullify undesirable factors with the lowest effect on the key performance parameters. In this way, in section 2, a brief declaration of performance will be stated alongside the targeted novelty. Then, section 3 will report electromagnetic outcomes that will show the

effectiveness of novelty and finally in section 4 salient achievement will be reviewed.

# 2 The nature of Operation and Implementation of Desired Topology

Fig. 1, showcases a 3D exploded view, revealing the dual stators, each with a U-shaped iron core, placed opposite each other. The PMs are aligned in a unidirectional orientation.

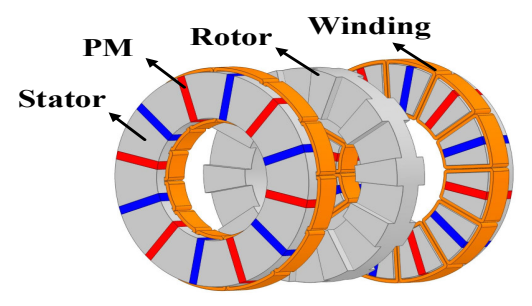
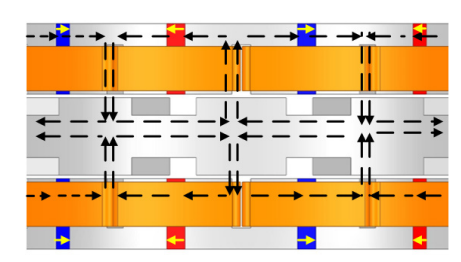


Fig. 1. Exploded view of the 12/10 poles AFFSPM.

Additionally, Fig. 2, presents a 2D model that depicts the flux paths. The rotor yoke acts as an intermediary, splitting the flux paths originating from the opposing magnets. The flux switching principal functions with changes in the rotor's position; when the rotor aligns with the magnet or teeth, a periodic electromotive force (EMF) and sinusoidal bipolar flux linkage are generated within the windings.



**Fig. 2.** Magnetization patterns as well as flux paths during switching.

To move on more to details, when the rotor pole aligns with the stator tooth, the flux undergoes switching, encompassing one-phase windings as they pass through the air gap. In the absence of excitation, part of the magnetic flux traverses the air gap while the rest creates a short circuit in the magnetic circuit. By applying sufficient positive current the excitation current generates magnetic flux, which, combined with the magnet flux, passes through the motor air gap, aiding in energy conversion. When the rotor pole reaches the next stator tooth, the flux direction through the air gap reverses.

The AFFSPM is constructed based on the theoretical framework and equations discussed below.

Initially, the general formula for output power is provided as follows [31]:

$$P_{out} = \frac{m}{2} E_m I_m \eta \tag{1}$$

where  $P_{out}$ , m and  $\eta$  indicate output power, phase number, and efficiency, respectively. Before calculating the maximum voltage  $(E_m)$  and current amplitudes  $(I_m)$ , the Back-EMF can be estimated using the following equations [31]:

$$e = -\frac{d\psi_m}{dt} = -N_{ph}\frac{d\varphi}{d\theta}\frac{d\theta}{dt} = -N_{ph}\frac{d\varphi}{d\theta}\omega_r;$$
 (2)

$$\varphi = \varphi_m \cos(P_r \theta)$$

where  $N_{ph}$ ,  $\omega_r$ ,  $\varphi_m$ ,  $P_r$ , and  $\theta$  denote the number of turns per winding in each phase, the rotor's angular speed, flux amplitude, rotor pole number, and rotor position angle, respectively. The subsequent equations individually express the Back-EMF and the amplitude of the sinusoidal current [32]:

$$E_{m} = N_{ph} \, \omega_{r} \, P_{r} \, K_{f} \, K_{l} \, B_{gmax} \, \beta_{s} \, \frac{\pi}{4P_{s}} \, (D_{o}^{2} - D_{i}^{2})$$
 (3)

$$I_{m} = \sqrt{2} I_{rms} = \frac{\sqrt{2}}{2} \frac{\pi A_{s} D_{i}}{m N_{ph}}$$
(4)

where  $P_s$  is the number of stator PMs,  $K_f$  is the flux leakage coefficient,  $K_l$  is related to the air gap flux density distribution,  $I_m$  represents the maximum current density,  $B_{gmax}$  indicates the peak air gap flux density,  $\beta_s$  is the area ratio of the stator tooth to the stator pole pitch, and  $D_o$  and  $D_i$  are the stator's outer and inner diameters, respectively.

Hence, power output can be defined as below [32]:

$$P_{out} = \frac{\sqrt{2} \pi^3}{240} \frac{P_r}{P_s} \eta K_f K_d \beta_s A_s B_{gmax} (1 - \lambda^2) D_o^3 n_r$$
 (5)

where  $K_d$  is the flux waveform distribution factor, and  $\lambda$  is the ratio of the stator's inner to outer diameter.

The motor's geometric parameters significantly influence the output torque.

In addition, it is essential to differentiate between CT and TR, where TR is a computational parameter that can be calculated for all types of machines as follows [33]:

$$TR(\%) = \frac{T_{max} - T_{min}}{T_{AVG}} \times 100 \tag{6}$$

while CT results from electromagnetic operation, derived from interactions with magnetic force, especially in salient structures. Faults can also contribute to creating ripples in electrical machines. The number and position of poles are key factors influencing CT and are not affected by loading or the armature's effect. Suitable approaches for reducing CT can be identified through its governing equations, which will be presented in further detail. The following equation gives a co-energy relation that evolved three terms [34]:

$$Wc = \frac{1}{2}Li^{2} + \frac{1}{2}R_{t}\varphi^{2} + \underbrace{f(i,\varphi)}_{flux-linkage \ and \ armature}$$
(7)

where L, I,  $R_t$ ,  $\varphi$  are inductance, current, air gap reluctance, and air gap flux linkage, respectively. In no-excited condition, the CT presented as:

excitedT=
$$-\frac{\partial W_C}{\partial \theta}$$
 no-ecited  $C=-\frac{1}{2}\varphi \frac{dR}{d\theta}$  (8)

here,  $W_C$  and  $\theta$  represent the co-energy and rotor position, respectively. According to this equation, the most effective way to reduce CT is by minimizing variations in air gap reluctance. It is evident that using a stronger magnet increases the air gap flux, and consequently, CT as well. Various techniques aim to reduce changes in reluctance throughout the structure. Alternatively, decreasing the harmonics of magneto motive force can also be a solution, though it may lead to a reduction in output torque.

Therefore, altering these parameters can affect not only the torque value but also the CT, vibration, and noise levels produced by the motor. This insight drives the introduction of a new design in this paper.

However, this article will focus on the variations in the rotor pole. Fig, 3. a, illustrates the 2D typical geometrical design of the stator and its PMs, while Common Pole (CP) structure is shown in Fig 3,b, [32]. The primary concept of this paper is to reverse the structure in the radial direction and evaluate the sensitivity of arc poles. Two parameters, namely the basic pole arc angle  $(\beta_r)$  and  $(\beta_f)$  the fan-shaped pole angle is introduced to create an RRP structure (Fig. 3.c) [35]. Additionally, the rotor pole arc without the fan-shaped pole will also be considered as the Basic Pole (BP) structure and evaluated further.

Given the structural limitations related to pole arc-topole pitch issues, Table 1 outlines the key parameters of the designed machine alongside the considered range for sensitive analysis.

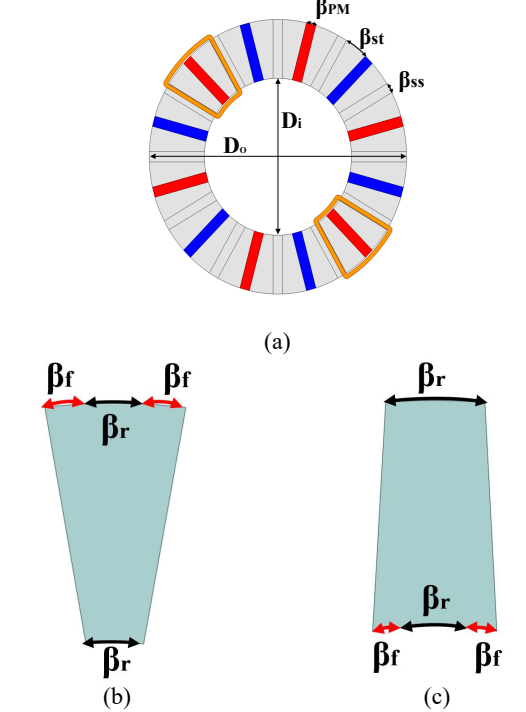


**Fig. 3.** 2D Up view of stator and PMs and its dimensions, (b) CP, (c) RRP.

**Table 1.** Key Dimension of the Conventional and Desired Motors.

Parameters	Value			
Rated output power (Pout)	600 W			
Rated speed (n <sub>r</sub> )	750 rpm			
Rated current (Is)	3.5 A			
Magnet remanence	1.2 T			
Turn per phase (Nph)	360			
Stator outer diameter (Do)	140 mm			
Stator inner diameter (Di)	80 mm			
Stator axial length (Ls)	20 mm			
Stator yoke length (Lsy)	8 mm			
Rotor axial Length (L <sub>r</sub> )	22 mm			
Machine axial length (La)	64 mm			
Stator tooth width $(\beta_{st})$	7.5 deg			
Stator slot width $(\beta_{ss})$	7.5 deg			
Stator PM width (β <sub>PM</sub> )	7.5 deg			
Rotor pole width (B <sub>r</sub> )	7.5 deg			
BP topology rotor pole	7.5			
Basic pole arc angles $(\beta_r)$	(2.5,5,7.5,10,12.5,15,17.5) deg			
Fan shape pole angles $(\beta_f)$	(0, 2, 4) deg			

# 3 Electromagnetic Evaluation

In this section, torque values are assessed across 35 distinct rotor pole configurations; Six values of  $(\beta_r)$  are evaluated under two modes of  $(\beta_f)$  for different structures. Additionally, torque values were measured for the same rotor pole dimensions at the highest and lowest positions.

To begin with, due to the importance of meshing on the electromagnetic results, Fig.4, demonstrates implemented meshes on the stator and rotor. Auto meshing with the surface element method is used.

The simulations performed in sinusoidal current excitation mode will be as shown in Fig. 5, with an amplitude close to 4.94 A and a frequency of 125Hz.

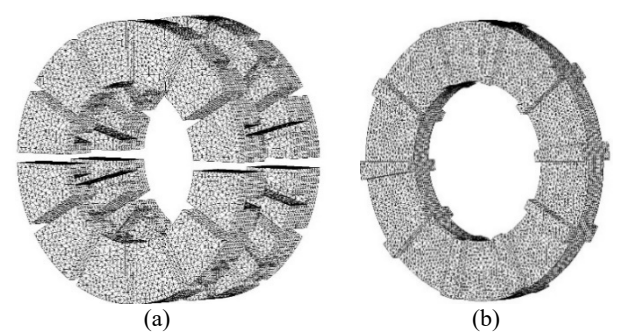


Fig. 4. 3D meshed parts: (a) stator, (b) rotor.

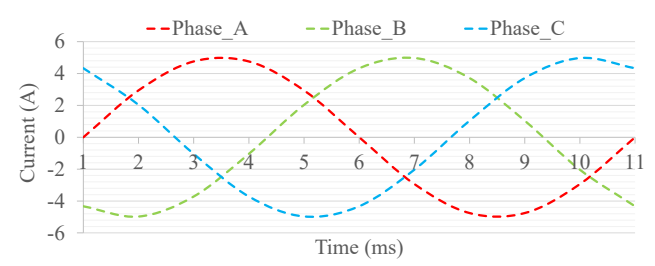


Fig. 5. Three-phase current profile.

To evaluate structures based on the torque characteristics, Table 2 shows the various modes in FEA and sensitivity analysis.

An observable trend indicates a smooth increase in torque as pole width increases, influenced by the two introduced parameters. Notably, the lowest torque value of 2.82 Nm was recorded for the model with  $(\beta_r=2.5)$  while the maximum torque was achieved in a similar structure without a fan shape at  $(\beta_r=12.5)$ .

For a constant  $\beta_f$ , as  $\beta_r$  increases, the torque trend initially rises, reaches a peak, and then decreases, suggesting an optimal point for  $\beta_r$ Values. This table also reveals that adding a fan shape reduces TR by creating a path with lower reluctance. Consequently, TR ranges from approximately 80% to about 10%.

Also, variations in CT, which range from 0.9 Nm to around 4 Nm have been reported in this table. In many cases, the addition of a fan shape reduces CT.

In this section, a performance evaluation criterion based on the ratio of AT to CT is used to identify the structure with optimal performance. Table 2 includes the results of these calculations for various scenarios. For an equitable comparison, the basic structure ( $\beta_f = 0$  and ( $\beta_r = 7.5$ ) is compared with two carefully chosen structures: one from the CP topology and another one from the RRP design. According to the results, the selected structure from the CP has ( $\beta_r = 4$ ) and ( $\beta_r = 12.5$ ), while the RRP structure has geometric

parameters including  $(\beta_r=4)$  and  $(\beta_r=15)$ . The calculated ratios of AT to CT for the CP and RRP structures were 8.32 and 7.73, respectively, compared to 3.81 for the basic topology without a fan shape. This indicates a clear improvement in the torque profile due to the use of a fan-shaped construction and, particularly, the reverse rotor pole configuration. Regarding the calculated ratios, a gradual increase in the coefficient with rising  $\beta_r$  is observed for the non-fan-shaped topology, but this trend does not apply to the other structures. In the rest of the paper, a comprehensive review will be done of the three chosen topologies in different terms.

**Table 2.** Torque Characteristics of the Presented Models.

Topology	Fan Shape Degree (βr)	CT (Nm)	AT (Nm)	AT/ CT (-)	TR (%)
	$\beta_r$ =2.5	2.37	2.82	1.18	73.95
	$\beta_r = 5$	3.86	4.33	1.12	80
	$\beta_r = 7.5$	1.83	6.99	3.81	27.1
BP	$\beta_r$ =10	1.8	6.77	3.76	28
	$\beta_{\rm r} = 12.5$	1.71	8.12	4.74	26.42
	$\beta_r$ =15	1.43	7.86	5.49	21.72
	$\beta_{\rm r} = 17.5$	0.89	6.88	7.73	27.05
	$\beta_r$ =2.5	3.5	4.81	1.37	72.72
	$\beta_r = 5$	1.19	6.18	5.19	25.55
	$\beta_{\rm r} = 7.5$	2.02	7.29	3.60	32.69
CP (βf=2)  CP (βf=4)  RRP (βf=2)	$\beta_r = 10$	1.33	7.49	5.63	21.9
	$\beta_{\rm r} = 12.5$	1.84	7.53	4.09	22.19
	$\beta_r$ =15	1.25	7.37	5.89	16.84
	$\beta_{\rm r} = 17.5$	2.15	6.72	3.12	31.98
	$\beta_{\rm r} = 2.5$	1.1	6.1	5.54	21.88
	$\beta_r = 5$	1.93	7.08	3.66	35
	$\beta_{\rm r} = 7.5$	1.43	7.9	5.52	22.28
	$\beta_r$ =10	1.31	7.6	5.80	19.93
	$\beta_{\rm r} = 12.5$	0.91	7.58	8.32	14.88
	$\beta_r$ =15	1.99	6.67	3.35	29.59
	$\beta_{\rm r} = 17.5$	1.09	5.69	5.22	26.77
	$\beta_r$ =2.5	1.66	3.79	2.28	45.58
	$\beta_r=5$	2.26	5.79	2.56	55.57
	$\beta_{\rm r}$ =7.5	1.16	7.08	6.10	13.18
	$\beta_r=10$	1.05	7.52	7.16	21.73
	$\beta_r$ =12.5	1.07	7.68	7.17	19.23
	$\beta_{\rm r}=15$	1.04	7.46	7.17	16.11
	$\beta_{\rm r}$ =17.5	1.18	6.85	5.80	18.14
	$\beta_r = 2.5$	1.6	4.8	3	26.82
	$\frac{\beta_r}{\beta_r}=5$	2.08	6.55	3.14	33.32
	$\beta_{\rm r}=7.5$	1.05	7.02	6.68	17
	$\frac{\beta_r}{\beta_r=10}$	1.19	7.83	6.57	23.54
	$\frac{\beta_{\rm r}}{\beta_{\rm r}=12.5}$	1.09	7.84	7.18	18.55
	$\beta_r = 15$	0.97	7.5	7.73	15.7
	$\beta_{\rm r} = 17.5$	0.84	6.45	7.67	24

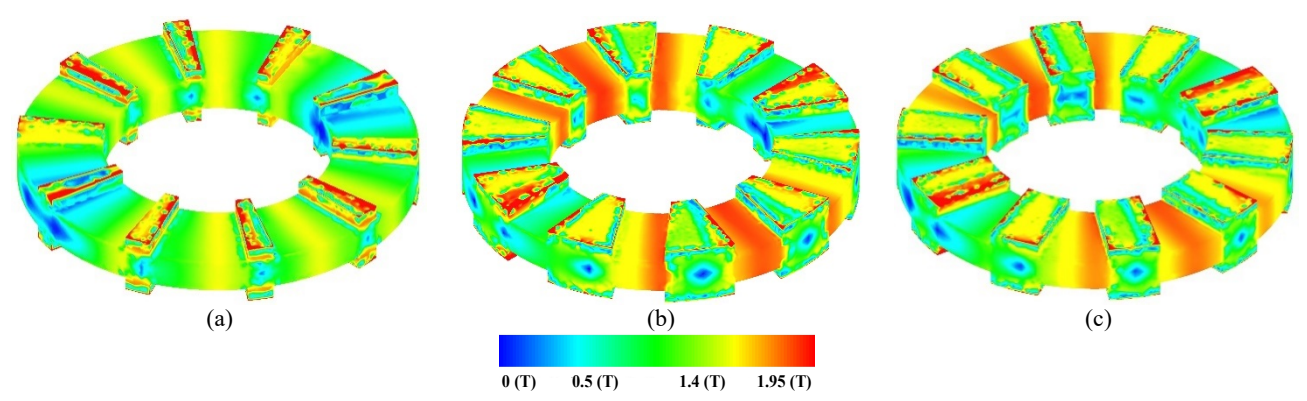


Fig. 6. Rotor flux density at the same rotor position for three selected topologies (a) BP ( $\beta_f = 0$ ,  $\beta_r = 12.5$ ), (b) CP ( $\beta_f = 4$ ,  $\beta_r = 12.5$ ), (c) RRP ( $\beta_f = 4$ ,  $\beta_r = 15$ ).

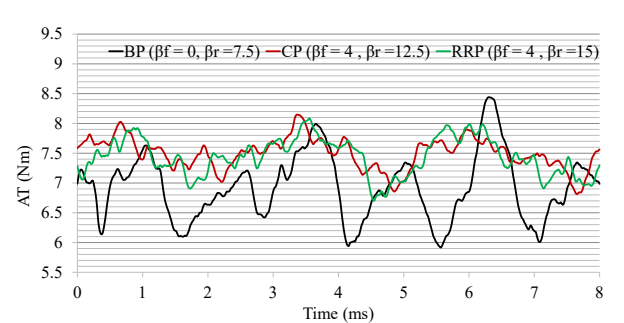
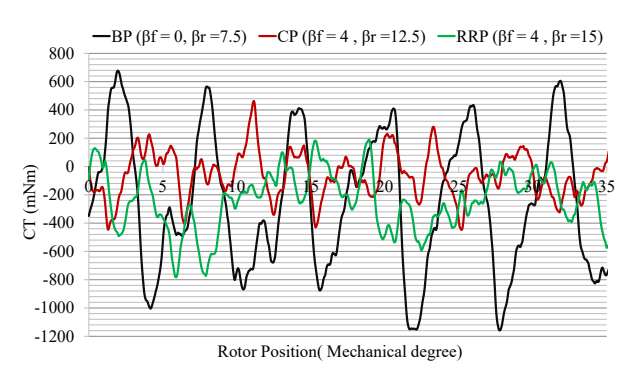


Fig. 7. AT in three selected topologies versus time.



**Fig. 8.** CT profiles in three selected topologies versus mechanical degrees.

Fig. 6, 10 illustrates the flux density distribution in the rotors. Overall, flux density values in the two structures with the proposed geometry have notably increased. The flux density change cycle across all structures remains consistent, although flux density values in the rotor yoke exhibit phase differences. In the basic rotor yoke configuration, the maximum recorded flux density is approximately 1.45 T, while in the two proposed structures, regions with higher flux paths show flux density values nearing the saturation limit of about 1.95 T. Torque profiles and CT profiles for three selected topologies are depicted in Fig. 7 and 8, respectively. Numerical details have already been covered, and the reduction in torque profile fluctuations within the proposed configurations is apparent. Additionally, the peak CT values have significantly decreased in both studied structures, ranging from approximately 1200 mNm to below 800 mNm and 400 mNm.

Moreover, the rate of change in the presented models is significantly greater than in the basic configurations.

Fig. 9, shows the Back-EMF voltages for all three structures in three different phases. Both proposed topologies exhibit a nearly similar increase in voltage components. In the BP structure, the effective back-EMF value is 48.5 V per phase, while this value is around 56.5 V in the CP and RRP models.

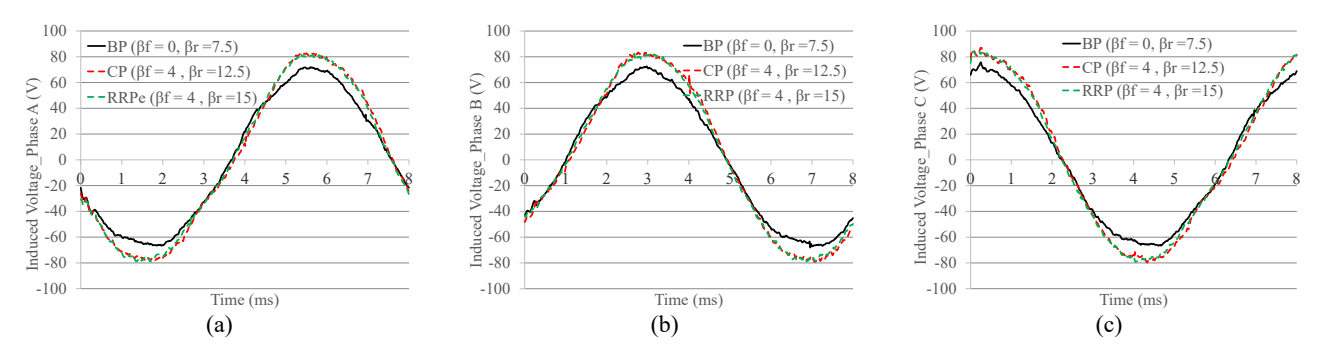


Fig. 9. Induced voltage in three different topologies for (a) Phase A, (b) Phase B, and (c) Phase C.

## 4 Conclusion

This paper explored an innovative design for an axialfield flux-switching machine, which includes a two-layer stator with 12 poles and a single 10-pole rotor. The primary goals were to enhance torque while reducing both cogging torque and torque ripple through structural changes. The rotor's straightforward and unique design allowed easy adjustments. The main innovation of this design is the radial reversal of the rotor pole compared to typical poles. Additionally, a fan-shaped geometric coefficient was introduced and its effects on the structure were analyzed. Finally, based on a coefficient representing the ratio of electromagnetic torque to cogging torque, three sample structures were compared. In the standard rotor pole structure, the average torque was 6.99 Nm, which increased to 7.58 Nm with the addition of fan-shaped rotor poles with different parameters. A similar increase was seen in the reverse rotor pole configuration. Furthermore, a significant reduction in cogging torque and torque ripple was observed. For the reverse rotor pole with specific geometry, the cogging torque decreased from 1.83 Nm to 0.9 Nm, and the torque ripple in both proposed structures was reduced by over 11%. The study demonstrates that the proposed method can enhance average torque while reducing torque ripple, improving the suitability of this machine type in various configurations

## References

- [1] H. Torkaman, A. Ghaheri, and A. Keyhani, "Design of Rotor Excited Axial Flux-Switching Permanent Magnet Machine," *IEEE Transactions on Energy Conversion*, vol. 33, no. 3, pp. 1175-1183, 2018.
- [2] J. Zhao, Q. Han, Q. Wang, L. Wang, and L. Wang, "Comprehensive Comparison of Stator-PM and Rotor-PM Axial Field PM Machines," *IEEE Transactions on Applied Superconductivity*, vol. 34, no. 8, pp. 1-6, 2024.
- [3] H. Ebrahimi, H. Torkaman, and H. Javadi, "Simultaneous improvement of cogging torque and torque density in axial fluxswitching permanent magnet motor," *IET Electric Power Applications*, vol. 18, no. 3, pp. 312-324, 2024.
- [4] A. G. Othman and A. E. Lashine, "Design and Performance Evaluation of an Axial Flux Switching Generator for a Wind Energy Conversion System," 22nd International Middle East Power Systems Conference (MEPCON), pp. 222-227, 2021.
- [5] P. Su, et.al., "Cogging Torque Reduction of Axial-Modular Flux Switching Permanent Magnet Machine by Module Combination Technique," *IEEE Transactions on Transportation Electrification*, vol. 10, no.1, pp. 1947 - 1956, 2024.
- [6] S. Wang et al., "Comparative Study of E- and U-core Modular Dual-Stator Axial-Field Flux-Switching Permanent Magnet Motors With Different Stator/Rotor-Pole Combinations Based on Flux Modulation Principle," *IEEE Access*, vol. 9, pp. 78635-78647, 2021.
- [7] A. Daghigh, H. Javadi, H. Torkaman, "Design Optimization of Direct-Coupled Ironless Axial Flux Permanent Magnet Synchronous Wind Generator With Low Cost and High Annual Energy Yield," *IEEE Transactions on Magnetics*, vol. 52, no. 9, pp. 1-11, Sept. 2016,.

- [8] M. A. Baig, J. Ikram, A. Iftikhar, S. S. H. Bukhari, N. Khan, and J. S. Ro, "Minimization of Cogging Torque in Axial Field Flux Switching Machine Using Arc Shaped Triangular Magnets," *IEEE Access*, vol. 8, pp. 227193-227201, 2020.
- [9] F. Farrokh, A. Vahedi, H. Torkaman, M. Banejad, A. J. Mahdi, and M. J. Mohammed, "Demagnetization and Fault-Tolerance Analysis in Dual-Stator Axial-Field Flux-Switching Permanent Magnet Motor," *IEEE Access*, vol. 12, pp. 102579-102591, 2024.
- [10] W. Zhang, H. Fan, K. Yao, J. He, and W. Xu, "Research on Efficiency Optimization Control Strategy of Axial Field Flux-Switching Permanent Magnet Motor," *IEEE Transactions on Industry Applications*, vol. 60, no. 4, pp. 6209-6221, 2024.
- [11] F. Farrokh, A. Vahedi, H. Torkaman, V. Z. Faradonbeh, M. S. Naghash, and M. Banejad, "Design of Axial-Field Flux-Switching PM Modular- Machine by The Approach of Identifying Suppressing Cogging Torque," in 3rd International Conference on Electrical Machines and Drives (ICEMD), 2023, pp. 1-5.
- [12] P. Kumar and R. K. Srivastava, "Cost-Effective Stator Modification Techniques for Cogging Torque Reduction in Axial Flux Permanent Magnet Machines," in *IEEE Transportation Electrification Conference and Expo, Asia-Pacific (ITEC Asia-Pacific)*, 2018, pp. 1-5.
- [13] A. Daghigh, H. Javadi, H. Torkaman, "Optimal Design of Coreless Axial Flux Permanent Magnet Synchronous Generator with Reduced Cost Considering Improved PM Leakage Flux Model." *Electric Power Components and Systems*, vol.45, no.3, pp. 264–278, 2016.
- [14] M. Aydin and M. Gulec, "Reduction of Cogging Torque in Double-Rotor Axial-Flux Permanent-Magnet Disk Motors: A Review of Cost-Effective Magnet-Skewing Techniques With Experimental Verification," *IEEE Transactions on Industrial Electronics*, vol. 61, no. 9, pp. 5025-5034, 2014.
- [15] D. Xu, M. Lin, X. Fu, L. Hao, and W. Zhang, "Influence of rotor design parameters on static characteristics of a novel Hybrid Axial Field Flux-Switching Permanent Magnet machine," in 17th International Conference on Electrical Machines and Systems (ICEMS), 2014, pp. 1096-1101.
- [16] M. Yousuf, F. Khan, J. Ikram, R. Badar, S. S. H. Bukhari, and J. S. Ro, "Reduction of Torque Ripples in Multi-Stack Slotless Axial Flux Machine by Using Right Angled Trapezoidal Permanent Magnet," *IEEE Access*, vol. 9, pp. 22760-22773, 2021
- [17] X. Y. Liang, W. Zhang, and H. H. Bao, "Influence of different stator cores on the electromagnetic performance of axial field flux-switching permanent magnet machines," in *IEEE International Conference on Applied Superconductivity and Electromagnetic Devices (ASEMD)*, 2015, pp. 126-127.
- [18] Z. Wei and L. Mingyao, "Influence of rotor pole number on optimal parameters in e-core axial field flux-switching permanent magnet machine," in *International Conference on Electrical Machines and Systems (ICEMS)*, 2013, pp. 1217-1221.
- [19] E. Yıldırız, M. Güleç, and M. Aydın, "An Innovative Dual-Rotor Axial-Gap Flux-Switching Permanent-Magnet Machine Topology With Hybrid Excitation," *IEEE Transactions on Magnetics*, vol. 54, no. 11, pp. 1-5, 2018.
- [20] C. Gan, J. Wu, M. Shen, W. Kong, Y. Hu, and W. Cao, "Investigation of Short Permanent Magnet and Stator Flux Bridge Effects on Cogging Torque Mitigation in FSPM Machines," *IEEE Transactions on Energy Conversion*, vol. 33, no. 2, pp. 845-855, 2018.
- [21] L. Hao, M. Lin, D. Xu, and W. Zhang, "Cogging Torque Reduction of Axial Field Flux-Switching Permanent Magnet Machine by Adding Magnetic Bridge in Stator Tooth," *IEEE Transactions on Applied Superconductivity*, vol. 24, no. 3, pp. 1-5, 2014.
- [22] A. B. Letelier, D. A. Gonzalez, J. A. Tapia, R. Wallace, M. A. Valenzuela, "Cogging Torque Reduction in an Axial Flux PM Machine via Stator Slot Displacement and Skewing," *IEEE Transactions on Industry Applications*, vol. 43, no. 3, pp. 685-693, 2007.

- [23] N. Li, J. Li, D. Xu, X. Hao, Q. Li, and M. Lin, "Cogging Torque Minimization of Axial Flux-Switching Permanent Magnet Machine via Rotor Teeth Skewing," in 24th International Conference on the Computation of Electromagnetic Fields (COMPUMAG), 2023, pp. 1-4.
- [24] A. N. Patel and B. N. Suthar, "Cogging Torque Reduction of Sandwiched Stator Axial Flux Permanent Magnet Brushless DC Motor using Magnet Notching Technique," *International Journal* of Engineering, vol. 32, no. 7, pp. 940-946, 2019.
- [25] Z. Xing, S. Han, C.-F. Dai, and Hua, "Study on the Electromagnetic Design and Analysis of Axial Flux Permanent Magnet Synchronous Motors for Electric Vehicles," *Energies*, vol. 12, p. 3451, 2019.
- [26] H. Torkaman and A. Sohrabzadeh, "Reduction of inappropriate principal features of the switched reluctance motor using sinusoidal rotor configuration," *IET Electric Power Applications*, vol. 18, no. 6, pp. 625-642, 2024.
- [27] H. Chen, D. Li, R. Qu, and T. Zou, "Torque Capacity Improvement of Flux-Switching PM Machines Based on Directional Stator Permeance Design," *IEEE Transactions on Industrial Electronics*, vol. 71, no. 5, pp. 4551-4561, 2024.
- [28] M. Babalou, H. Torkaman, E. Pouresmaeil, N. Pourmoradi, "Fault Tolerant Dual Active Bridge Converter for Electric Vehicle Application." *Iranian Journal of Electrical and Electronic Engineering*, vol. 20, no. 2, 2024.
- [29] J. Zhao, X. Quan, X. Tong, and M. Lin, "Cogging Torque Reduction in Double-Rotor Hybrid Excited Axial Switched-Flux Permanent Magnet Machine," *IEEE Transactions on Applied Superconductivity*, vol. 30, no. 4, pp. 1-5, 2020.
- [30] L. Mo, T. Zhang, and Q. Lu, "Thermal Analysis of a Flux-Switching Permanent-Magnet Double-Rotor Machine With a 3-D Thermal Network Model," *IEEE Transactions on Applied Superconductivity*, vol. 29, no. 2, pp. 1-5, 2019.
- [31] F. Farrokh, A. Vahedi, H. Torkaman, M. Banejad, "Design and comparison of dual-stator axial-field flux-switching permanent magnet motors for electric vehicle application," *IET Electrical Systems in Transportation*, vol. 13, no. 2, p. e12074, 2023.
- [32] M. Lin, L. Hao, X. Li, X. Zhao, and Z. Q. Zhu, "A Novel Axial Field Flux-Switching Permanent Magnet Wind Power Generator," *IEEE Transactions on Magnetics*, vol. 47, no. 10, pp. 4457-4460, 2011.
- [33] A. Sohrabzadeh, H. Torkaman, and E. Afjei, "Torque Ripple Reduction and Radial Force Mitigation in the Switched Reluctance Motor Using a Novel Rotor Configuration," in 14th Power Electronics, Drive Systems, and Technologies Conference (PEDSTC), 2023, pp. 1-4.
- [34] O. Kudrjavtsev and A. Kilk, "Cogging torque reduction methods," in *Electric Power Quality and Supply Reliability Conference (PQ)*, 2014, pp. 251-254.
- [35] H. Ebrahimi, H. Torkaman, A. Sohrabzadeh, A. Jaferian, and H. Javadi, "Reverse Rotor Pole Construction in Axial-Field Flux-Switching PM Machine with High-Torque and Low-Cogging Torque" 4rd International Conference on Electrical Machines and Drives (ICEMD), 10-11 Dec. 2024, Tehran, Iran, pp. 1-6.



Hamid Ebrahimi received the B.Sc. degree in electrical engineering, in 2007, and the M.Sc. degree, in 2010, with a focus on fault diagnosis of induction. He is currently pursuing a Ph.D. degree in electrical engineering with the Faculty of Electrical Engineering, Shahid Reheshti University, Tehran, Iran. His research interests include the electromagnetics design, thermal and analysis, optimization, manufacturing of electric machines, with a focus on flux switching, axial field PM, and flywheel energy storage systems..



Hossein Torkaman (Senior Member, IEEE) is an Associate Professor in the Faculty of Electrical Engineering at Shahid Beheshti University, Tehran, Iran. He also serves as the head of the electrical machines and converters design research center laboratory. He has authored over 200 peer-reviewed journal and conference papers and holds five granted patents. He is the author of seven books and has been the recipient of numerous awards and research grants from both academic institutions and industry partners. His research interests focus on electrical machines, power electronics and renewable energy systems...



Alireza Sohrabzadeh received his B.Sc and M.Sc degrees in electrical engineering from the University of Kashan and Shahid Beheshti University, in 2020 and 2022. He is a research assistant at the Electrical Machines and Converters Design Research Center at Shahid Beheshti University. His main fields of interest are electrical machines, power electronics, magnetic gears and renewable energies.



Hamid Javadi is currently an Associate Professor in the Faculty of Electrical Engineering, Shahid Beheshti University, Tehran, Iran. He has published more than 50 technical papers in journal articles and conference proceedings. His main research interests include power electronics, electrical machines, and high voltage engineering.